BJP BRITISH JOURNAL OF PHARMACOLOGY

BPS BRITISH PHARMACOLOGICAL SOCIETY

British Journal of Pharmacology (2009), 158, 1720–1734
© 2009 The Authors
Journal compilation © 2009 The British Pharmacological Society All rights reserved
0007-1188/09
www.brjpharmacol.org

RESEARCH PAPER

Thalidomide attenuates nitric oxide-driven angiogenesis by interacting with soluble guanylyl cyclase

Syamantak Majumder[1], Megha Rajaram[1], Ajit Muley[1], Himabindu S Reddy[1], KP Tamilarasan[1], Gopi Krishna Kolluru[1], Swaraj Sinha[1], Jamila H Siamwala[1], Ravi Gupta[1], R Ilavarasan[2], S Venkataraman[2], KC Sivakumar[4], Sharmila Anishetty[3], Pradeep G Kumar[4] and Suvro Chatterjee[1]

[1]*Vascular Biology Lab, AU-KBC Research Centre, Anna University, Chennai, TN, India,* [2]*Department of Pharmacology, C. L. Baid Metha College of Pharmacy, Thorapakkam, Chennai, TN, India,* [3]*Centre for Biotechnology, Anna University, Guindy Campus, Chennai, TN, India and* [4]*Molecular Reproduction Unit, Rajiv Gandhi Centre for Biotechnology, Trivandrum, Kerala, India*

Background and purpose: Nitric oxide (NO) promotes angiogenesis by activating endothelial cells. Thalidomide arrests angiogenesis by interacting with the NO pathway, but its putative targets are not known. Here, we have attempted to identify these targets.

Experimental approach: Cell-based angiogenesis assays (wound healing of monolayers and tube formation in ECV304, EAhy926 and bovine arterial endothelial cells), along with *ex vivo* and *in vivo* angiogenesis assays, were used to explore interactions between thalidomide and NO. We also carried out *in silico* homology modelling and docking studies to elucidate possible molecular interactions of thalidomide and soluble guanylyl cyclase (sGC).

Key results: Thalidomide inhibited pro-angiogenic functions in endothelial cell cultures, whereas 8-bromo-cGMP, sildenafil (a phosphodiesterase inhibitor) or a NO donor [sodium nitroprusside (SNP)] increased these functions. The inhibitory effects of thalidomide were reversed by adding 8-bromo-cGMP or sildenafil, but not by SNP. Immunoassays showed a concentration-dependent decrease of cGMP in endothelial cells with thalidomide, without affecting the expression level of sGC protein. These results suggested that thalidomide inhibited the activity of sGC. Molecular modelling and docking experiments revealed that thalidomide could interact with the catalytic domain of sGC, which would explain the inhibitory effects of thalidomide on NO-dependent angiogenesis.

Conclusion and implications: Our results showed that thalidomide interacted with sGC, suppressing cGMP levels in endothelial cells, thus exerting its anti-angiogenic effects. These results could lead to the formulation of thalidomide-based drugs to curb angiogenesis by targeting sGC.

British Journal of Pharmacology (2009) **158,** 1720–1734; doi:10.1111/j.1476-5381.2009.00446.x; published online 13 November 2009

Keywords: angiogenesis; thalidomide; soluble guanylate cyclase; cGMP; nitric oxide

Abbreviations: BAEC, bovine aortic endothelial cells; 8Br-cGMP, 8-bromo cyclic guanosine monophosphate; CAM, chorio-allantoic membrane; cGMP, cyclic guanosine monophosphate; EC, endothelial cell; ENL, erythema nodosum leprosum; eNOS, endothelial nitric oxide synthase; NOS, nitric oxide synthase; PDE, phosphodiesterase; PI, propidium iodide; SC, sildenafil citrate; sGC, soluble guanylate cyclase; SNP, sodium nitroprusside

Introduction

The resurgence of thalidomide in the treatment of various diseases represents an unprecedented pharmaceutical renaissance. It is not only used successfully in the treatment of refractory multiple myeloma (Pearson and Vedagiri, 1969). but has also been implicated in the treatment of cutaneous lupus, scleroderma and Crohn's disease (Wilhelm *et al.*, 2006). This immunomodulatory agent was first synthesized in 1954 to treat morning sickness among pregnant women (Randall, 1990). It was banned due to its teratogenic effects during the 1960s, and subsequently made a re-appearance in 1998 when the Food and Drug Administration approved it as a treatment

Correspondence: Dr Suvro Chatterjee, Vascular Biology Lab, AU-KBC Research Centre, MIT Campus, Anna University, Chennai 600 044, Tamil Nadu, India. E-mail: soovro@yahoo.ca
Received 24 April 2009; revised 22 May 2009; accepted 31 May 2009

for erythema nodosum leprosum (ENL), a subtype of leprosy. More recently, thalidomide was approved for the treatment of multiple myeloma and has shown efficacy in a wide range of malignant and non-malignant diseases (Melchert and List, 2007).

In the early 1990s, thalidomide was first reported to exhibit potent anti-angiogenic properties, which was said to be responsible for the teratogenic effects on limb buds observed in offspring of thalidomide exposed mothers (D'Amato *et al.*, 1994). Research on thalidomide has largely focused on its immunomodulatory effects, although it possesses several anti-angiogenic effects as well. Angiogenesis can be attenuated in several ways, including inhibition of vascular endothelial growth factor (VEGF) and interleukin (IL)-6. However, these are not necessarily exclusive (Corral and Kaplan, 1999). In our previous study, we demonstrated that thalidomide modified migration of endothelial cells (ECs) by interfering with the nitric oxide (NO) pathway, before any indicative tube structure had been formed (Tamilarasan *et al.*, 2006). Although thalidomide is known to down-regulate VEGF and basic fibroblast growth factor (bFGF), the mechanism of thalidomide-mediated inhibition of angiogenesis is not fully understood.

Cellular NO, a second messenger, plays a central role in mediating angiogenesis and is produced by the action of one of the three isoforms of NO synthase (NOS). NO initiates a downstream cascade of events by stimulating the synthesis of cGMP. In response to pro-angiogenic stimulation, angiotensin I and phosphoinositol-3 kinase activate endothelial NOS (eNOS) and thus NO production (Sessa, 2004). We found that thalidomide interfered with the migration of EC by blocking NO signalling (Tamilarasan *et al.*, 2006), and we have sought, here, to further analyse this action of thalidomide. The aim of the present study was to identify putative targets of thalidomide action in the NO pathway, and to characterize their interactions with thalidomide.

Methods

Cell culture

We used an immortalized human umbilical vein EC line (ECV 304), which has been identified as a bladder cancer-derived EJ1/T24 cell by STR–PCR analysis (Brown *et al.*, 2000). The ECV 304 cell line was used as a representative of cancerous ECs, and was cultured in Dulbecco's modified Eagle's medium (DMEM) supplemented with 10% fetal bovine serum (FBS) (v/v) and 1% penicillin (w/v) and streptomycin (w/v). Another immortalized endothelial hybrid cell line, EAhy926, used as a representative of normal immortalized EC, was from Dr C.J.S. Edgell. These cells were cultured in DMEM supplemented with 10% FBS (v/v) and 1% penicillin (w/v) and streptomycin (w/v) (Matsuda *et al.*, 1997). We also used primary cultures of bovine EC (see below).

Primary cell culture

The bovine aortic EC (BAECs) were isolated from the aorta of freshly slaughtered cattle from a government-authorized abbatoir. The aorta was collected aseptically and placed in phosphate-buffered saline (PBS) (pH 7.4) for transport to the laboratory. In the laboratory, vessels were washed with PBS, and connective tissue and fat were removed aseptically. Next, ECs were harvested as described elsewhere (Ryan, 1984). Isolated cells were confirmed as ECs by using antibodies against endothelial markers, eNOS and factor VIII respectively. The cells were used for experiments until passage 6.

Animals

Animal care was in accordance with national, local and institutional guidelines. The Institutional Animal Care and Use Committee of C. L. Baid Metha College of Pharmacy approved all experimental animal procedures. All procedures were performed in the animal facility at Department of Pharmacology, C. L. Baid Metha College of Pharmacy, Thorapakkam, Chennai, TN, India. Six-week-old male Wistar rats were caged in groups of three to six rats with free access to chow and water. The animal room was kept constantly at 26°C, 38.5% humidity, with a 12 h light–12 h dark cycle.

Wound healing assay

ECV 304, EAhy926 or BAEC were trypsinized and seeded on collagen-plated 24-well plates with 80% cell density. Twenty-four hours later, when the cells reached confluency, the EC monolayer was scratched with a 1 mm wide sterile plastic scraper to make a linear 'wound'. As described elsewhere (Staton *et al.*, 2004), the cells were washed with PBS and incubated with thalidomide for 8 h. Bright field images were taken with 4× magnifications under an inverted microscope. To study the cross talk between thalidomide and the NO downstream pathway, we used 50 μM 1H-[1,2,4]-oxadiazolo[4,3-a]quinoxalin-1-one (ODQ) (concentration from Majumder *et al.*, 2007; Kolluru *et al.*, 2008); a haem site inhibitor of soluble guanylyl cyclase (sGC); and 10 μM LY83583 (concentration from Millette and Lamontagne, 1996), a reversible inhibitor of sGC. Further, to evaluate the effects of external cGMP administration on thalidomide-treated cells, we incubated ECs with 50 μM 8Br-cGMP (concentration from Majumder *et al.*, 2007; Kolluru *et al.*, 2008), an analogue of cGMP, and 10 μM sildenafil citrate (SC; concentration from Majumder *et al.*, 2007; Kolluru *et al.*, 2008), an inhibitor of phosphodiesterase (PDE)-5 for 8 h. To check reversal of thalidomide's effects on ECs by NO donors, we used 500 μM of sodium nitroprusside (SNP; concentration from Tamilarasan *et al.*, 2006; Kolluru *et al.*, 2008). YC1, an NO independent activator of sGC (100 mM; concentration from Wohlfart *et al.*, 1999) was also employed. All additions were made after 30 min of pretreatment with thalidomide. The rate of wound healing was quantified from the images using Scion Image, release alpha 4.0 3.2 and Adobe Photoshop version 6.0.

Endothelial ring formation assay

Ring formation experiments were performed using the protocol mentioned elsewhere (Majumder *et al.*, 2007). ECV 304 cells (10^4 cells) were seeded on collagen (collagen type I)

in 24-well plates. After 12 h of incubation, the cells were pretreated with thalidomide for 30 min, and then SNP was added to the cells and incubated for a further 12 h. ODQ or LY83583 were used to assess the role of NO in the effect of thalidomide on endothelial ring formation. The effect of 8Br-cGMP on ring formation in thalidomide-treated EC monolayers was also studied. The number of rings formed in the monolayer was counted under bright field phase contrast microscope. The number of rings formed under SNP treatment was considered as 100%, and other values were expressed relative to this.

Three-dimensional (3D) tube formation assay in Matrigel
In this study, 1×10^4 ECV304 cells were grown in 24-well plates coated with Matrigel. The cells were treated with thalidomide, thalidomide + 8Br-cGMP or thalidomide + SC. The cells were incubated for 24 h, and the number of tubes formed was counted.

Angiogenesis pit formation assay
ECV304 cells were grown in 24-well plate coated with Matrigel and incubated for 24 h. After 24 h, the ECs gathered together in 100–150 μ patches to form pits, which dig into the 3D matrigel surface. The mouth of the wide-open pit is lined by a ring, two cells wide, which gives an impression of the wall of the well (Figure 1B). This wall is represented as vessel wall. Once the pits are formed, they were treated with thalidomide and thalidomide + 8Br-cGMP for another 24 h. Finally, images were taken under 20× magnification to analyse the structural integrity and number of the pits.

Measuring apoptosis using propidium iodide (PI) incorporation assay
PI has been widely used for the evaluation of apoptosis in different experimental systems (Srinivas *et al*., 2003), characterizing apoptotic cells by the pattern of DNA fragmentation. The experiments were performed using EAhy926 cells, as described earlier (Srinivas *et al*., 2003).

In another set of experiment, EAhy926 cells were treated with 0, 25, 50 and 75 $\mu g \cdot mL^{-1}$ of thalidomide for 4 h and fixed with 2% paraformaldehyde followed by permeabilization with 0.1% Triton X-100 for 2 min. The cells were then incubated with 1 $\mu g \cdot mL^{-1}$ of PI for 30 min. After incubation, the cells were washed gently and fluorescent images of the cells were acquired under 60× oil immersion objective using DP71 camera adapted to an Olympus IX71 microscope.

Annexin V measurement using annexin V–FITC apoptosis detection kit
EAhy926 cells were grown overnight in Petri dishes and treated with 75 $\mu g \cdot mL^{-1}$ of thalidomide for 4 h. Treated cells were then processed using the protocol supplied by the manufacturer (Merck, Calbiochem, EMD Chemicals Inc., Darmstadt, Germany). Fluorescence images of the cells were taken, and the numbers of annexin V–FITC-positive cells were counted per field.

cGMP measurement using enzyme immunoassay kit
Levels of intracellular cGMP were measured using the cGMP enzyme immunoassay kit supplied by Sigma (St Louis, MO, USA). ECV304 or EAhy926 cells were treated with thalidomide for 4 h. In another set of experiments, the cells were pretreated with thalidomide for 30 min followed by SNP treatment for 4 h. The treated cells were then processed by the protocol supplied by the manufacturer.

Egg yolk angiogenesis assay
Chicken eggs incubated for 4 days were collected from the Poultry Research Station, Nandanam, Chennai. The eggs were broken and gently placed in Petri dishes under sterile conditions. Paper discs, soaked in thalidomide solution (with and without 8Br-cGMP) were then placed on the egg yolks, which were incubated for another 12 h. Images were taken in 2× and 4× magnification using Nikon Cool Pix camera (Olympus India Pvt Ltd, New Delhi, India) adapted to a stereomicroscope at 0, 6 and 12 h of incubation. Images were analysed using Angioquant software (Niemistö *et al*., 2005).

Cotton plug and sponge–Matrigel plug angiogenesis assay in Wistar rats
Sterile absorbent cotton wool plugs (10 mg cotton wool per plug) were soaked in with various concentrations of thalidomide or thalidomide + 8Br-cGMP solutions, and were implanted subcutaneously the front left groin in rats. After 7 days, granulomas were excised and closed-up images were taken. Then, these tissue samples were extracted in saline for 3–4 h, and haemoglobin in the saline extracts was measured by the absorbance at 532 nm.

Foam sponges (polyethersulphone; 10×5 mm) were soaked in Matrigel containing thalidomide or thalidomide + 8Br-cGMP, and incubated for gelatinization for 15 min at 37°C. After gelatinization, sponge–Matrigel plugs were implanted subcutaneously in rats. After 7 days, the granulomas were excised and closed-up images were taken using a Nikon Cool Pix camera. Haemoglobin in the granulomas was extracted and measured spectrophotometrically, as described earlier.

Assay of sGC–thalidomide interactions by the pull-down method
Thalidomide in experimental samples was measured by its fluorescence (excitation/emission of 291/398 nm using Varian Carry eclipse fluorescence spectrophotometer , Varian, Inc., Palo Alto, CA, USA) in water : acetonitrile (80:20) solvent (pH 5 with 1 mM nitric acid solution), using a standard curve (0–100 $\mu g \cdot mL^{-1}$) (Cardoso *et al*., 2003).

To assay thalidomide–sGC interactions, 10^8 cells were seeded in tissue culture plates and incubated overnight. Protein A sepharose micro-beads were incubated over night at 4°C in 1:100 dilution of polyclonal primary antibody (IgG) against β subunit of sGC in order to allow antibody–bead adhesion. Cells were treated with 75 $\mu g \cdot mL^{-1}$ of thalidomide and incubated for 8 h. After treatment, the cells were washed three to four times with PBS and lysed using the lysis buffer [Tris–HCl 50 mM, ethylenediaminetetraacetic acid (EDTA) 0.1 mM, ethylene glycol tetraacetic acid 0.1 mM, sodium

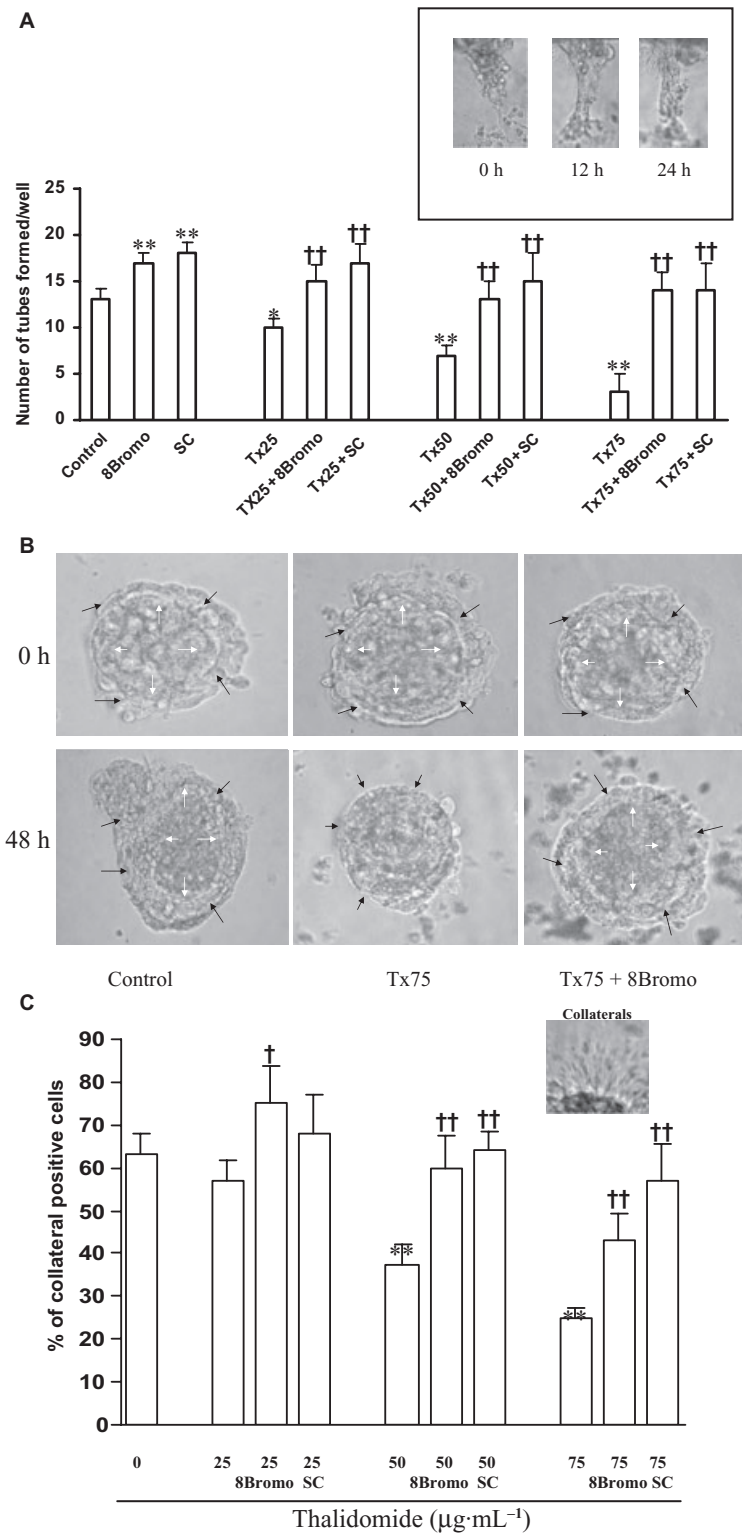

Figure 1 Thalidomide blocks 3D assembly of endothelial cell (EC) in Matrigel by interacting with the nitric oxide (NO)–cGMP pathway. (A) ECV304 cells were grown in Matrigel-coated 24-well plates and treated with thalidomide for 30 min. Formation of tubes in the cultures was inhibited by thalidomide, and these effects were reversed by adding 8Br-cGMP or sildenafil citrate (SC). Note that 8Br-cGMP or SC alone elevated 3D tube formation by ECV304 cells. *$P < 0.05$ and **$P < 0.001$ versus control, ††$P < 0.001$ versus Tx-treated sets ($n = 7$). (B) Pits formed by ECV304 cells on Matrigel were treated with thalidomide or thalidomide + 8Br-cGMP. Images were taken before and after 24 h of treatment, and revealed development of the pit boundary and the interior furrow. Thalidomide alone attenuated development of the pit boundaries and combination with 8Br-cGMP partially reversed thalidomide-induced inhibition. Images are representative of five different sets of experiments. (C) Pits were treated with thalidomide for 30 min followed by 8Br-cGMP or SC. After 24 h, the number of cells with collateral extensions was counted. Thalidomide inhibited formation of collaterals and combining 8Br-cGMP or SC with thalidomide partially reversed this inhibition collateral formation by the endothelial pits. **$P < 0.001$ versus control, †$P < 0.05$ and ††$P < 0.001$ versus Tx-treated sets ($n = 7$).

dodecyl sulphate 1%, deoxycholate 0.1%, NP-40 1%, pH 7.5]. Antibody-absorbed protein A micro-beads were then incubated overnight at 4°C with the cell lysates in order to pull down sGC from the samples. The samples were then centrifuged at 2300× *g* for 5 min. Next, the beads were incubated with 0.1% trypsin–EDTA solution for 30 min in 37°C in order to release sGC-bound thalidomide. The samples were then centrifuged at 9000× *g* for 10 min in order to pellet the beads. Then, aqueous acetonitrile (see above) was added to the sample, and the fluorescence of the sample was measured at excitation/emission of 291/398 nm. Control experiments were performed by using IgG coated beads + thalidomide, cells + IgG uncoated beads and thalidomide-treated cells + IgG uncoated beads. Total protein concentration of each sample was measured by Lowry's method, and the data obtained were normalized.

Immunofluorescence analysis
These studies were carried out on EAhy926 cells in 12-well plates using the cold paraformaldehyde–Triton X-100 procedures (Mukhopadhyay *et al.*, 2006). Cells were incubated at 4°C overnight with mouse monoclonal antibodies (dilution 1:1000) against sGC. Next, corresponding goat anti-mouse secondary antibodies (dilution 1:2000) tagged with FITC were used. Images were collected using an Olympus IX71 epifluorescence microscopy system equipped with a DP71 camera.

Western blot analysis
ECV304 cells were treated with different concentrations of thalidomide, and incubated for 8 h and harvested for Western blot analysis (Laemmli, 1970). Total protein concentration was normalized using the biuret assay and UV absorption of the protein sample. Proteins were detected by using 1:500 dilution of sGC β1 antibody (H79, Santa Cruz, CA, USA) and 1:1000 dilutions of goat anti-rabbit IgG conjugated to horseradish peroxidase (Bangalore GENEI, Bangalore, India). The blots were developed by using TMB/H_2O_2 as substrate. Loading control was the expression level of β-actin gene.

Homology modelling, docking and interatomic contact analysis
The primary sequence of sGC large subunit α (accession no. NP_000847.2) was used for searching sequences of known 3D structures at Expasy. The following templates 1yk9A.pdb (p = 2e-24), 1tl7A.pdb (p = 7e-22), 1cjtA.pdb (p = 7e-22), 1azsA.pdb (p = 7e-22) and 2gvdA.pdb (p7e-22) which got high $P(N)$ scores were used for generating the homology model of sGC residues 471–633. Iterative template fitting, raw sequence alignment and refinement used Promod II (version 3.7) (Peitsch, 1996). The structure of thalidomide (CID5426) was retrieved from Pubchem Compounds database.

The refined homology model of sGC was used for docking experiments with thalidomide using Autodock (Morris *et al.*, 1998) software. The top-ranked complex was saved in a PDB (Berman *et al.*, 2000) format for further analysis.

To ascertain the contacts between sGC and thalidomide, interatomic contact analysis of the *in silico* complex was performed using interatomic contact analysis option of WHAT IF modelling package (Vriend, 1990). This utility computes distances between atoms in a PDB structure/complex. Two atoms are said to be in contact if the distance between their van der Waals surfaces is less than 1.0 Å. A more stringent measure defines a contact when the distance between the van der Waals surfaces of the two atoms is less than 0.25 Å. In our evaluation, we have used both the options.

InterPro domains (Apweiler *et al.*, 2001), Pfam domains (Finn *et al.*, 2008) and Prosite motifs (Hulo *et al.*, 2006) of sGC α-subunit were obtained from the SwissProt database (Bairoch and Apweiler, 2000) entry to find conserved domains mapping to different regions of this subunit.

Statistical analysis. All the experiments were performed in triplicate (n = 3) unless otherwise specified. Data are presented as mean ± SEM. Data were analysed using one-way analysis of variance test, Student's t-test and Tukey *post hoc* tests as appropriate. Values of $P \leq 0.05$ were selected as showing a statistically significant difference.

Materials
DMEM was purchased from PAN biotech, Aidenbach, Bavaria. FBS was from Invitrogen Life Technologies (Carlsbad, CA, USA). Thalidomide, SNP, 8-bromo-guanosine-3′5′-monophosphate (8Br-cGMP), ODQ, 3-(5′-hydroxymethyl-2′-furyl)-1-benzyl indazole (YC-1), SC, cGMP enzyme immunoassay kit, PI were purchased from Sigma Chemical Co. 6-Anilino-5,8-quinoline quinone (LY83583), annexin V–FITC apoptosis detection kit and antibodies were purchased from Calbiochem, EMD Chemicals Inc. Matrigel was purchased from BD Biosciences, Becton Drive, NJ, USA. Foam sponges were from Amersham Bioscences, Sunnyvale, CA, USA. All other chemicals were of the reagent grade and were obtained commercially.

Results

Thalidomide blocked NO-induced ring formation in EC
To explore the effect of thalidomide on NO-induced ring formation, ECV304 cells were treated with thalidomide for 30 min. SNP (500 μM) was then added to the media to assess NO-induced reversal of thalidomide's effects. The number of rings formed in control and SNP-treated cultures was significantly reduced by 75 $\mu g \cdot mL^{-1}$ thalidomide (Figure 2A). This reduction was concentration dependent with respect to thalidomide over the range tested (25, 50 and 75 $\mu g \cdot mL^{-1}$). However, SNP treatment only reversed the inhibition in cells treated with 25 $\mu g \cdot mL^{-1}$ thalidomide.

Effects of sGC inhibitors on thalidomide-induced inhibition of ring formation in EC
NO has been shown to act via the NO–cGMP pathway to modulate endothelial responses (Ignarro, 1991). Thus, the ECV304 cells were treated first with thalidomide, and subsequently with LY83583, a reversible inhibitor of sGC, and SNP (Figure 2B). Either thalidomide or LY83583 or the combination decreased the formation of rings. SNP was not able to

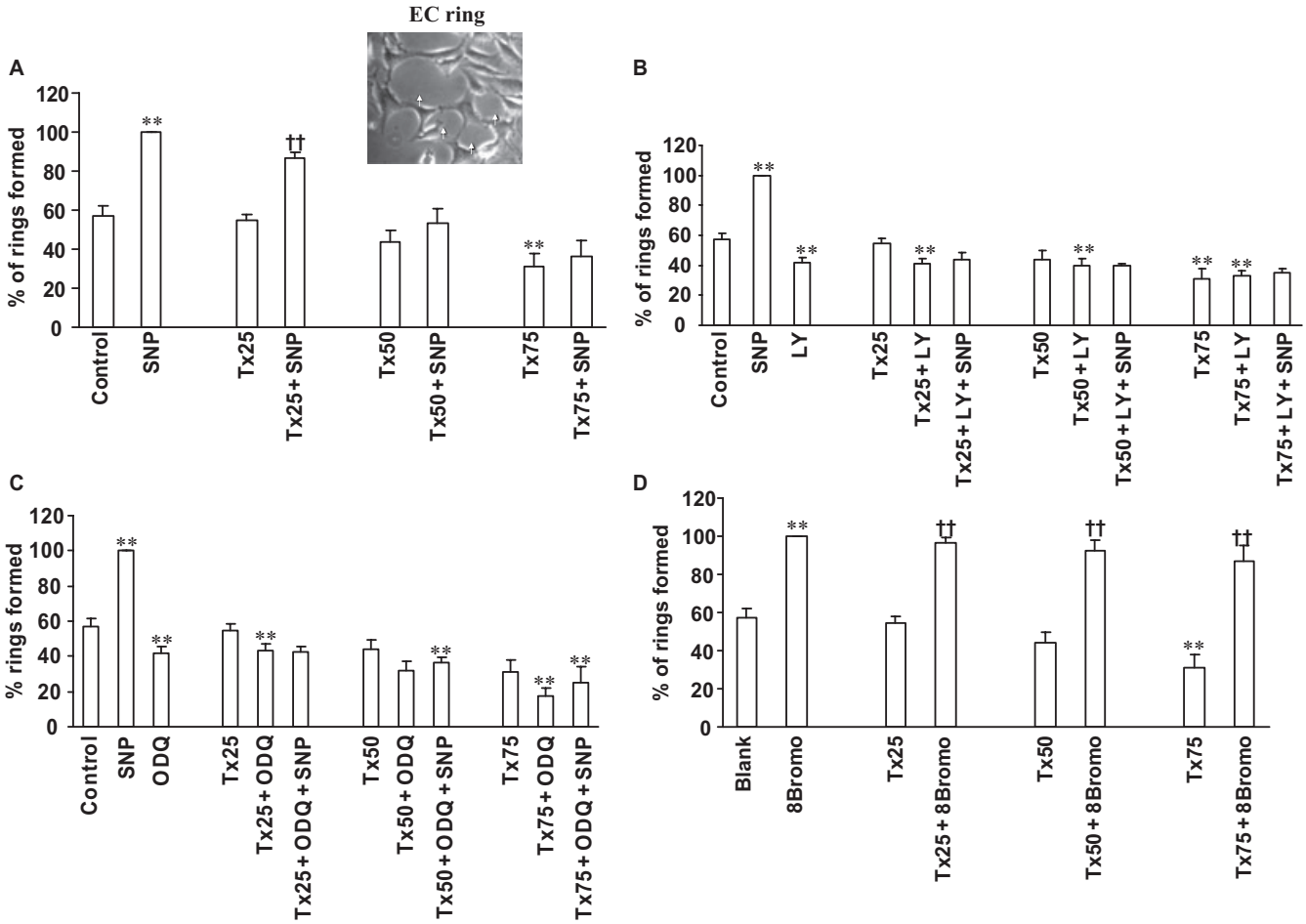

Figure 2 Thalidomide interacts with the nitric oxide (NO)–cGMP pathway to arrest ring formation in endothelial cell (EC) cultures. (A) ECV304 cells were treated with thalidomide (25, 50 and 75 $\mu g \cdot mL^{-1}$; Tx25, Tx50, Tx75) for 30 min. Sodium nitroprusside (SNP) was then added to cells and incubated for another 12 h. Thalidomide (75 $\mu g \cdot mL^{-1}$) significantly inhibited ring formation and exogenous NO (as SNP) did not reverse thalidomide-induced block of ring formation. $^{**}P < 0.001$ versus control, $\dagger\dagger P < 0.001$ versus Tx25 treated set ($n = 7$). (B) ECV304 cells were treated with thalidomide for 30 min followed by LY83583 (LY), SNP or the combination (LY83583 + SNP) treatment for 12 h. Thalidomide, LY83583 or the combination blocked ring formation. SNP failed to reverse the effects of thalidomide + LY83583 on endothelial ring formation. $^{**}P < 0.001$ versus control ($n = 7$). (C) ECV304 cells were treated with thalidomide for 30 min followed by SNP, 1H-[1,2,4]-oxadiazolo[4,3-a]quinoxalin-1-one (ODQ) or their combination for 12 h. SNP increased ring formation by EC while ODQ, a reversible inhibitor of sGC, and the combined treatment (thalidomide + ODQ) blocked ring formation. SNP did not reverse the effects of the combination. $^{**}P < 0.001$ versus control ($n = 7$). (D) ECV304 cells were treated with thalidomide for 30 min followed by 8Br-cGMP for 12 h. Addition of 8Br-cGMP totally reversed the effects of thalidomide. Note that 8Br-cGMP alone increased ring formation by EC. $^{*}P < 0.05$ and $^{**}P < 0.001$ versus control. $\dagger\dagger P < 0.001$ versus Tx-treated sets ($n = 5$).

reverse the inhibition due to the combination of thalidomide + LY83583 (Figure 2B). These results showed that, in the presence of an sGC inhibitor, the NO donor SNP was not able to reverse the effects of thalidomide.

A similar set of experiment was performed to evaluate the effects of ODQ, a haem site inhibitor of sGC. Again, thalidomide, ODQ or the combination, reduced formation of rings as compared to control and SNP-treated cultures (Figure 2C). SNP partially reversed the inhibitory effects of 50 and 75 $\mu g \cdot mL^{-1}$ thalidomide + ODQ (Figure 2C).

8Br-cGMP reversed the inhibitory effects of thalidomide on ring formation

To evaluate the effects of raising cGMP in thalidomide-treated cells, ECV304 cells were incubated with 50 μM 8Br-cGMP, a cell-permeant analogue of cGMP. This concentration of 8Br-cGMP completely prevented the inhibition of ring formation, at all concentrations of thalidomide (Figure 2D). Note that 8Br-cGMP alone increased ring formation in ECV304 cells.

8Br-cGMP and SC reversed thalidomide-induced inhibition of EC functions in Matrigel matrix

ECV304 cells form tubes when cultured on a Matrigel matrix. Whereas incubation with 8Br-cGMP or SC alone increased the number of tubes formed per well, thalidomide, at all three concentrations, inhibited tube numbers (Figure 1A). This effect of thalidomide was reversed when either 8Br-cGMP or SC was added to the cultures (Figure 1A).

ECV304 cells cultured on Matrigel will also form pits with a defined wall (see methods; Figure 1B). Incubation for 24 h

with thalidomide (75 μg·mL^{-1}) caused breakdown of these pit walls and thereby reduced the effective diameter of the pits. Adding 8Br-cGMP protected the wall of these pits from the damage caused by thalidomide treatment (Figure 1B).

ECV304 cells have a natural tendency to organize themselves to form conduit-like structures in Matrigel monolayer culture. We observed that these conduits further give rise to collateral extensions of cells, which develop into capillary-shaped structures. These functions of ECV304 cells can be quantified by measuring the proportion of cells with collateral extensions. Incubation with thalidomide (50 or 75 μg·mL^{-1}) decreased this proportion, and such inhibition was reversed by adding either 8Br-cGMP or SC to the thalidomide-treated cultures (Figure 1C).

Modulation of effects of thalidomide on 'wound healing' in EC monolayers

Cultures of EC can be 'wounded' by scratching the monolayer, and 'healing' takes place by re-growth of EC into the wound. This healing in ECV304 monolayers was inhibited by thalidomide, concentration dependently (Figure 3A), and addition of SC to the thalidomide-treated cultures reversed this inhibition. Note that SC alone increased healing in control cultures.

In a similar model of wound healing in EAhy926 cells and primary cultures of BAEC, thalidomide (75 μg·mL^{-1}) also suppressed wound healing. This suppression was reversed by adding 8Br-cGMP, but not SNP, although both of these compounds were able to increase healing in control cultures (Figure 3B).

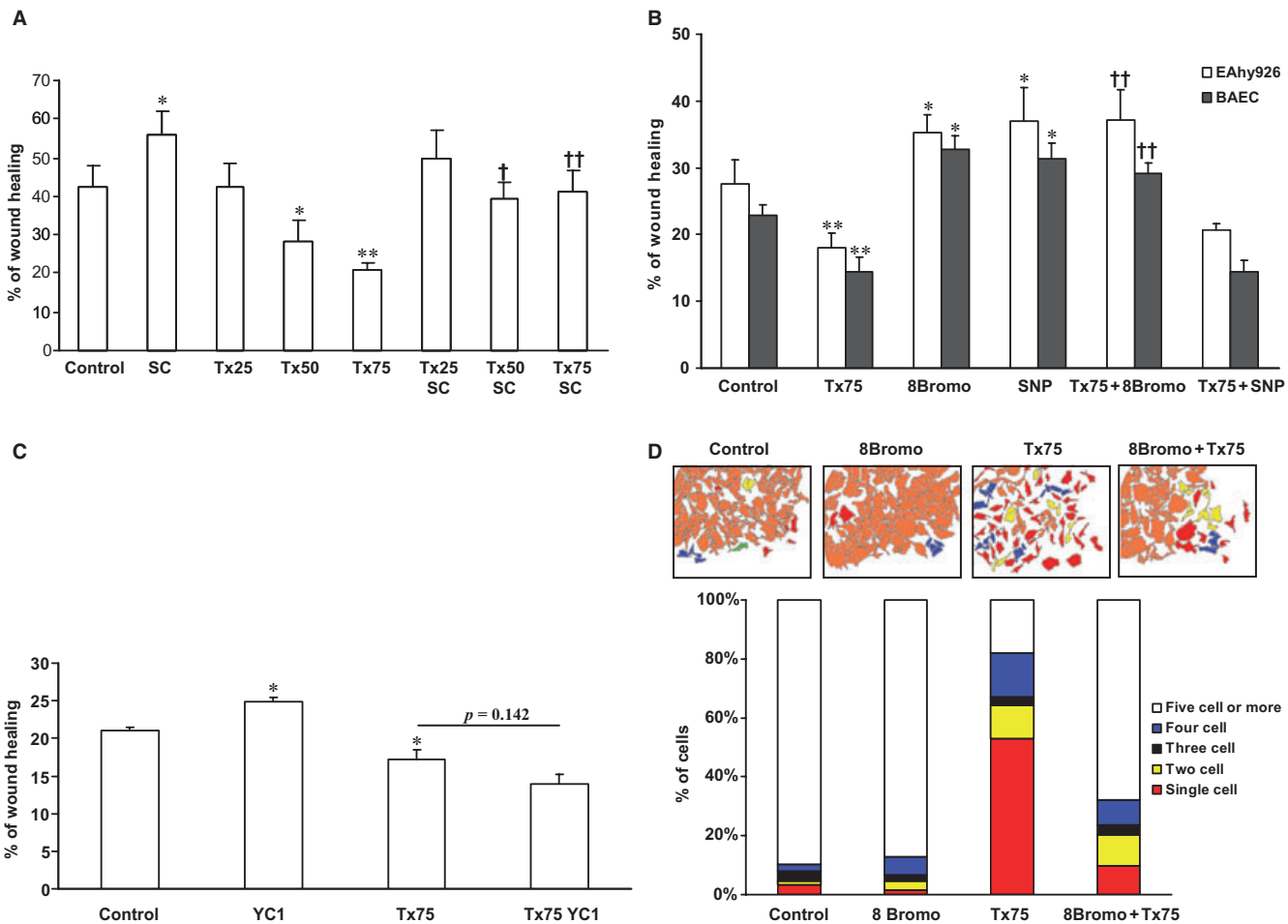

Figure 3 Thalidomide blocks the nitric oxide (NO)–cGMP pathway to inhibit endothelial migration and cell clustering. (A) A scratch was made in endothelial cell monolayers to create a 'wound'. Wounded monolayers were treated with thalidomide for 15 min, then sildenafil citrate (SC) was added and wound healing was tracked for the next 8 h. SC alone increased, whereas thalidomide alone (50 and 75 μg·mL^{-1}) blocked endothelial wound healing. Adding SC to thalidomide partially reversed the inhibition of wound healing. *P < 0.05 and **P < 0.001 versus control, †P < 0.05 and ††P < 0.001 versus Tx-treated sets (n = 5). (B) Wounds in EAhy926 and and BAEC monolayers were treated with thalidomide and sodium nitroprusside (SNP) or 8Br-cGMP was added. Thalidomide blocked the migration of cells, while 8Br-cGMP or SNP alone facilitated endothelial wound healing. Combined treatment with thalidomide + 8Br-cGMP restored wound healing, but SNP did not reverse the effects of thalidomide. *P < 0.05 and **P < 0.001 versus control. ††P versus Tx-treated sets (n = 5). (C) Wounds in EAhy926 monolayers were treated with thalidomide, YC-1 or in combination. YC-1 alone increased, while thalidomide blocked, wound healing. However, YC-1 failed to reverse the inhibitory effect of thalidomide. *P < 0.05 versus control (n = 5). (D) Wounds in EAhy926 monolayers were treated with thalidomide or thalidomide + 8Br-cGMP for 8 h. Bright field images were taken and were processed to identify clusters of cells (as described in Methods). Five different colours were assigned to indicate numbers of cells in a cluster. The number of single cells was increased by thalidomide treatment and adding 8Br-cGMP reversed this effect (n = 3).

Using EAhy926 cells, the effects of YC-1, a direct, non-NO-mediated activator of sGC, on wound healing was assessed (Figure 3C). By itself, YC-1 did increase wound healing in control cultures, but, when added to thalidomide-treated cultures, this compound did not reverse the effects of thalidomide.

A time lapse imaging of the edges of the wound in EAhy926 cells showed that cells were organized in clusters with different numbers of cells in each cluster. The number of cells in each of the clusters was counted and is presented as a percentile bar diagram in Figure 3D. Under control conditions, most of the clusters (more than 80%) contain five or more cells, and this contrasts with the distribution in thalidomide-treated cultures where such clusters have fallen to about 20%, with many more single cells at the edge of the wound. Adding 8Br-cGMP to thalidomide-treated cultures largely reversed these effects of thalidomide (Figure 3D).

Thalidomide induced apoptosis in EC

Thalidomide increased the number of apoptotic, PI-positive, EAhy926 cells concentration dependently (Figure 4A). Fragmentation of the genomic DNA was detected using PI to stain fixed permeabilized EAhy926 cells. Intact nuclei were observed in control cultures, while in thalidomide-treated cultures there was an equal distribution of intact and fragmented nuclei (Figure 4B). Further assessment of apoptotic EAhy926 cells was made with Annexin V–FITC apoptosis detection kits. As shown in Figure 4C, thalidomide treatment increased the proportion of cells positive for annexin V–FITC.

8Br-cGMP reversed thalidomide-induced anti-angiogenic effects in ex vivo and in vivo models

The egg yolk vascular bed provides a well-accepted, *ex vivo*, angiogenesis model (Tufan and Satiroglu-Tufan, 2005). Thalidomide exhibited anti-angiogenic effects in this model which were reversed by adding 8Br-cGMP (Figure 5A,B; Table 1).

Another *in vivo* model of angiogenesis uses cottonwool plugs and sponge–Matrigel plugs implanted subcutaneously in rats. After 7 days of implantation, the rats were killed and the plugs were removed. The extent of angiogenesis was determined by assaying the haemoglobin content of the plug implants. There was a marked inhibition of angiogenesis (haemoglobin content) after thalidomide treatment (Figure 6) which was reversed by adding 8Br-cGMP to the implant along with thalidomide.

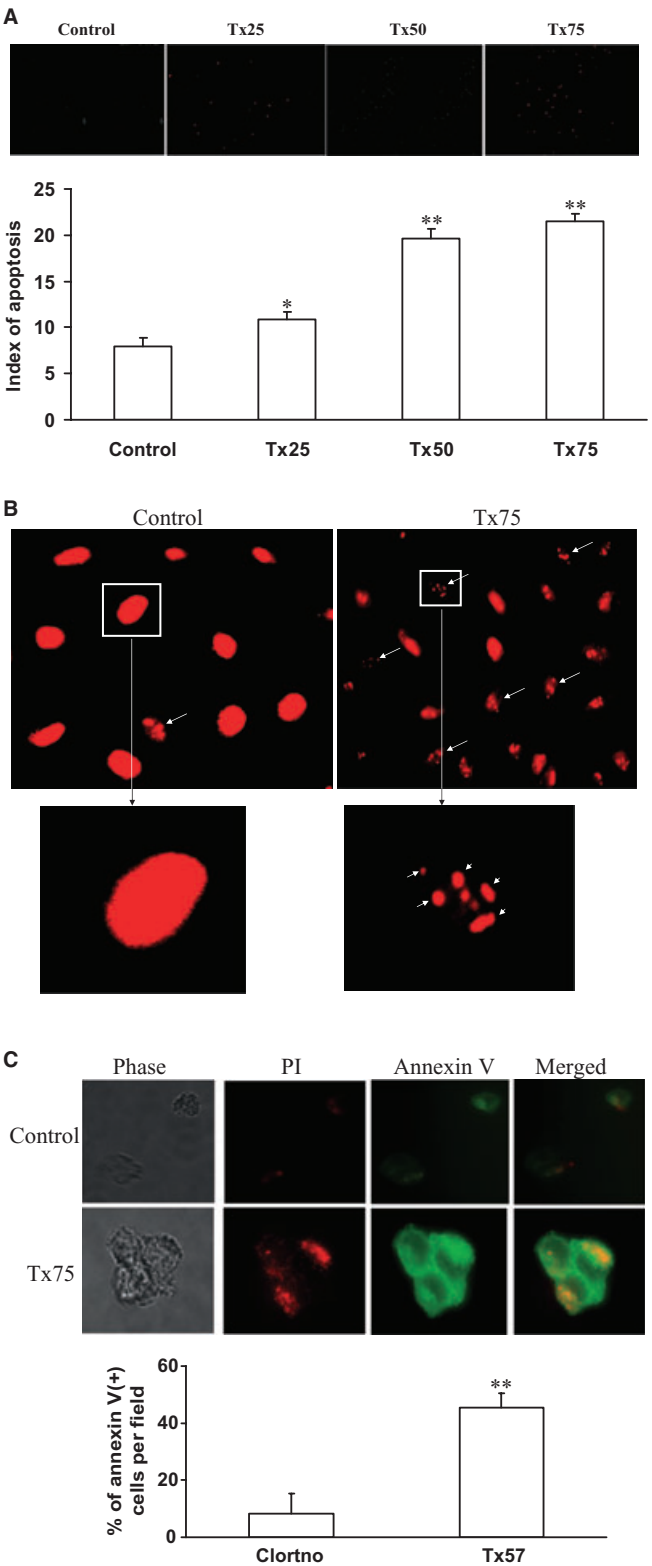

Figure 4 Thalidomide induced apoptosis in endothelial cell (EC). (A) Thalidomide-treated EAhy926 cultures were examined for the presence of apoptotic cells. Fluorescent images of the propidium iodide (PI)-positive, red nuclei were taken as an index of apoptosis. The number of PI-positive cells was increased concentration dependently by thalidomide. *$P < 0.05$ and **$P < 0.001$ versus control ($n = 7$). (B) In a similar set of experiments, the EAhy926 cells were treated with thalidomide, fixed, permeabilized and stained with PI. Fragmentation of nuclear material was observed after thalidomide treatment. Images are the representative of five different sets of experiments. (C) The EAhy926 cells were treated with thalidomide, and apoptotic cells were detected using the annexin V–FITC apoptosis detection kit. The images are representative of four individual experiments. **$P < 0.001$ versus control ($n = 3$).

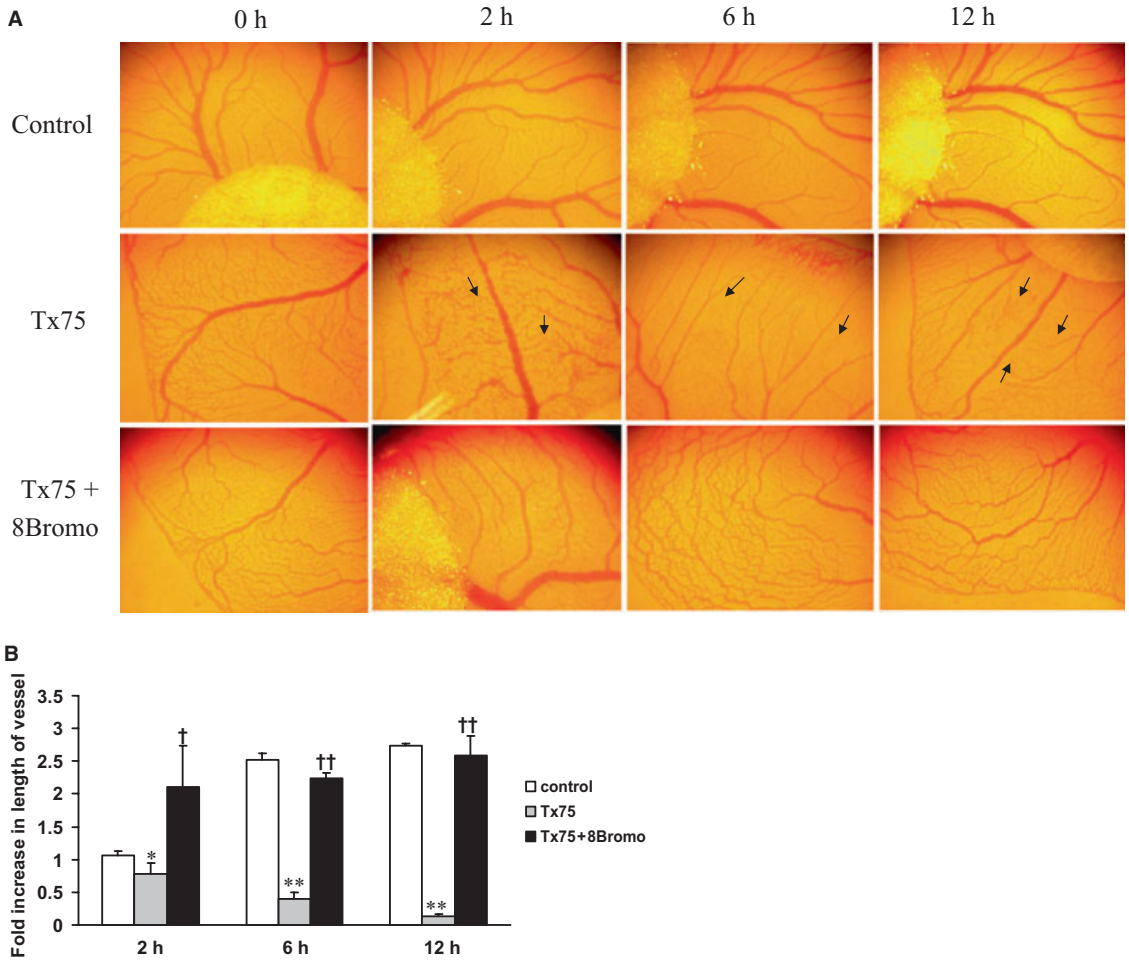

Figure 5 Thalidomide interacts with the nitric oxide (NO)–cGMP pathway to arrest *ex vivo* angiogenesis. (A) Sterilized paper discs soaked in thalidomide (75 μg·mL^{-1}), were placed on the egg yolk vascular bed for 30 min. Next, 8Br-cGMP was added to the disc and incubated for another 12 h. There was a marked inhibition of angiogenesis with thalidomide treatment at all the time points. Adding 8Br-cGMP partially reversed this thalidomide-induced inhibition of angiogenesis. Images are representative of three different sets of experiments. (B) Images of the egg yolk were then analysed using Angioquant image analysis software. Data extracted from this analysis showed inhibition of *ex vivo* angiogenesis with thalidomide treatment, while adding 8Br-cGMP partially restored the angiogenesis. *$P < 0.05$ and **$P < 0.001$ versus control, †$P < 0.05$ and ††$P < 0.001$ versus Tx-treated sets ($n = 3$).

Table 1 Pattern of angiogenesis in egg yolk assay with thalidomide treatment

Type of experiment		*Time (hours)*		
		2 h	*6 h*	*12 h*
Control	Complex	2.02 ± 0.04	5.71 ± 0.19	7.39 ± 0.34
	Length	1.06 ± 0.06	2.51 ± 0.10	2.73 ± 0.03
	Size	1.10 ± 0.07	2.12 ± 0.09	2.10 ± 0.16
	Junctions	0.84 ± 0.09	2.28 ± 0.14	2.81 ± 0.21
Thalidomide	Complex	0.74 ± 0.05	0.66 ± 0.08	0.41 ± 0.09
	Length	0.77 ± 0.17	0.39 ± 0.10	0.13 ± 0.03
	Size	1.01 ± 0.06	0.39 ± 0.05	0.20 ± 0.04
	Junctions	0.78 ± 0.10	0.32 ± 0.07	0.20 ± 0.09
Thalidomide + 8Bromo	Complex	1.15 ± 0.20	1.56 ± 0.27	1.63 ± 0.30
	Length	2.1 ± 0.63	2.24 ± 0.07	2.59 ± 0.30
	Size	2.49 ± 0.29	2.53 ± 0.09	3.04 ± 0.09
	Junctions	1.62 ± 0.20	2.46 ± 0.09	2.63 ± 0.30

Thalidomide blocked *ex vivo* angiogenesis which 8Br-cGMP reversed. The egg yolk angiogenesis assay was performed with thalidomide or thalidomide + 8Br-cGMP treatment. Images were taken after 0, 2, 6 and 12 h incubation. After 12 h, the number of vessel complexes, vessel length, vessel size and number of vessel junctions were reduced after thalidomide alone, but adding 8Br-cGMP reversed these changes. Experiments were performed in triplicate, and data are presented as mean ± SEM.

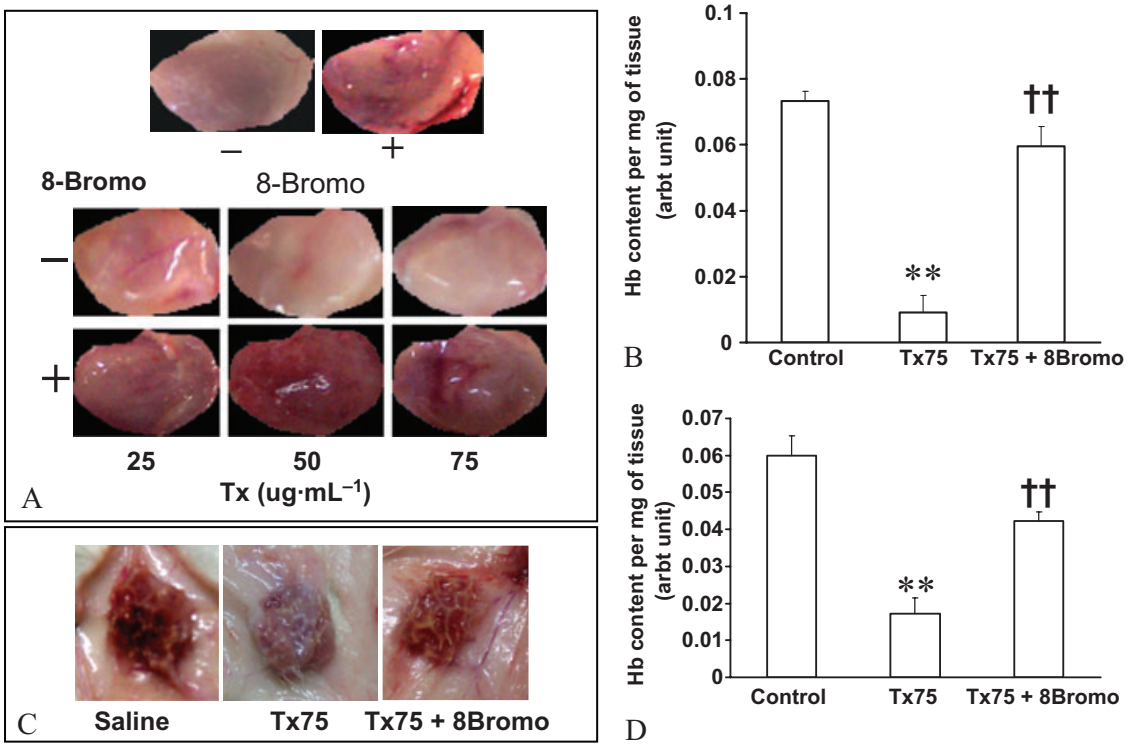

Figure 6 Thalidomide blocked *in vivo* angiogenesis through a cGMP-dependent pathway. *In vivo* angiogenesis experiment was measured using cotton and sponge–Matrigel plugs, soaked in thalidomide or 8Br-cGMP solutions, implanted subcutaneously in rats. After 7 days, the granulomas formed by the plugs were taken out. 8Br-cGMP alone in the implants promoted *in vivo* angiogenesis, while thalidomide alone inhibited angiogenesis. Combining 8Br-cGMP with thalidomide restored angiogenesis in both cotton and sponge–Matrigel plug models. $^{**}P < 0.001$ versus control, $\dagger\dagger P < 0.001$ versus Tx-treated sets ($n = 3$).

Table 2 Modelling of thalidomide docking with human soluble guanylyl cyclase

	Distance cut-off of 0.25 angstrom	*Distance cut-off of 1 angstrom*
Thalidomide	Leu 506, Ser 560, Asp 561, Val 563, Met 564, Glu 569, Pro 570, Ile 571.	Ile 487, Leu 506, Leu 509, Ser 560, Asp 561, Val 563, Met 564, Glu 569, Pro 570, Ile 571, Lys 572.

Thalidomide exerted its effect by interacting with different residues of the catalytic domain of human sGC. The table shows the residues of the catalytic domain of human sGC that could potentially interact with thalidomide. Interatomic contact analysis of the *in silico* complexes was performed using interatomic contact analysis option of WHAT IF modelling package to check the interaction of thalidomide with sGC. This utility computes distances between atoms in a PDB structure/complex. Two atoms are said to be in contact if the distance between their van der Waals surface is less than 1.0 Å. A more stringent measure defines a contact when the distance between the van der Waals surface of the two atoms is less than 0.25 Å.

Thalidomide decreased cellular cGMP levels in EC

Based on our results in the tube formation and wound healing assays, it was likely that thalidomide exerted its effects by modulating cellular cGMP levels. We therefore measured cellular cGMP in ECV304 cells and observed a concentration-dependent fall in the levels of cGMP after incubation with thalidomide (Figure 7A). We also investigated the levels of cGMP in EAhy926 cells. Here, thalidomide decreased cGMP in control cultures and in those stimulated with SNP. Note that SNP alone elevated cGMP formation in EAhy926 cells (Figure 7B).

A fall in cellular cGMP could be due to a decreased level of sGCc. We therefore measured the levels of sGC by immunofluorescence in whole cells and by Western blots in cell extracts, with ECV304 and EAhy926 cells. As shown in Figure 7C,D, treatment of cultures induced no differences in the expression levels of sGC either in whole cells (Figure 7C) or in Western blots of cell extracts (Figure 7D).

Thalidomide binds to sGC in EC

Possible binding of thalidomide to sGC was assessed by pull-down experiments, using protein A beads coated with rabbit anti sGC (β-subunit) IgG to extract sGC from cell lysates, with subsequent assessment of the thalidomide by fluorimetry. Pull down of sGC from samples of thalidomide-treated cultures had 60% more thalidomide fluorescence than those from control cultures ($P = 0.024$). This result indicates that thalidomide did physically interact with sGC in EC cultures.

Modelling of thalidomide binding to the potential catalytic region of sGC

We used *in silico* methods to model possible binding sites for thalidomide in sGC. The homology model of the catalytic domain of sGC shows a prominent substrate-binding cavity.

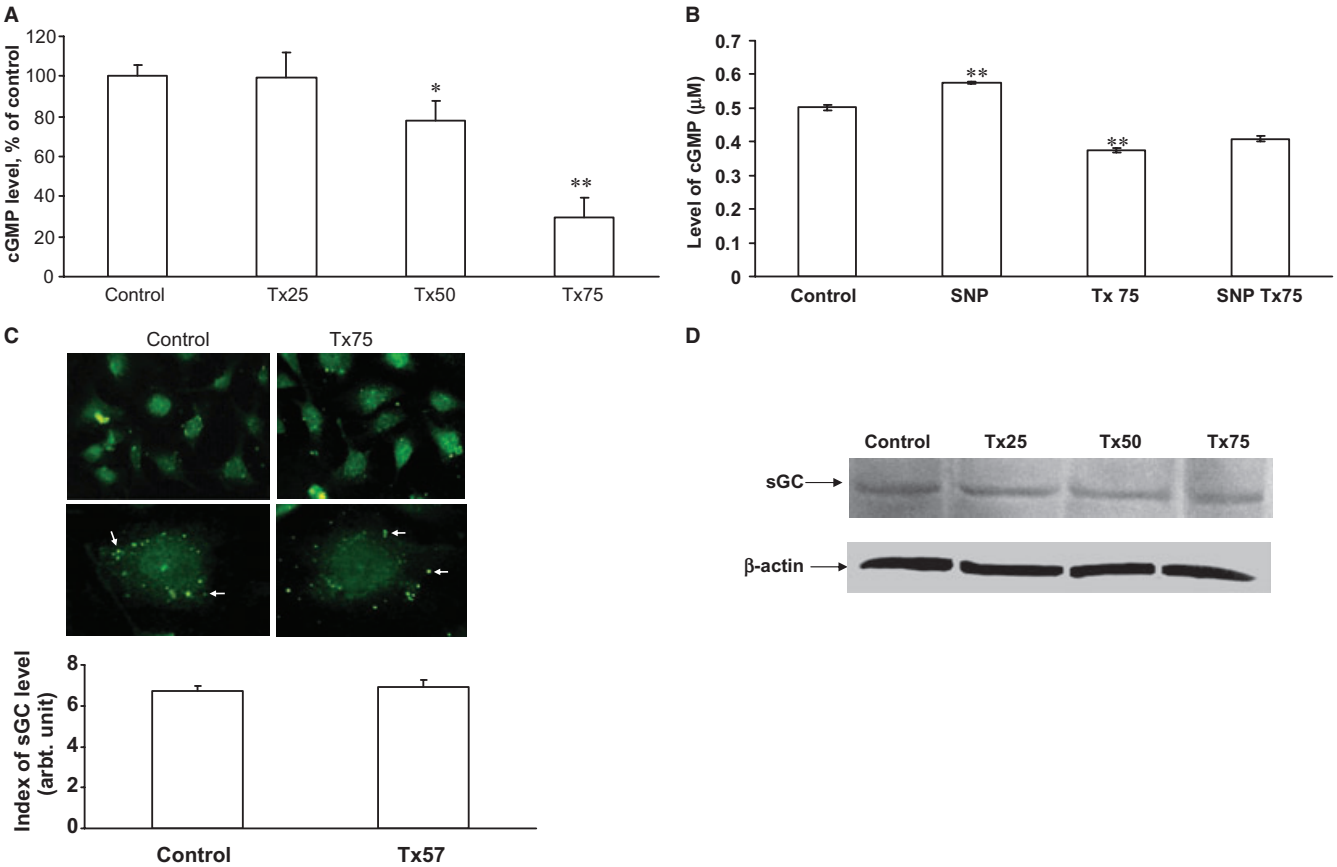

Figure 7 Thalidomide reduced cellular cGMP levels, but not the expression level of soluble guanylyl cyclase (sGC). (A) Levels of cGMP in ECV304 cells were measured after treatment with thalidomide. There was a concentration-dependent decrease in the cGMP level. *$P < 0.05$ and **$P < 0.001$ versus control ($n = 5$). (B) EAhy926 cells were incubated with thalidomide for 30 min followed by sodium nitroprusside (SNP) for 4 h. Next, cGMP levels in treated cells were evaluated using cGMP enzyme immunoassay kit. Thalidomide inhibited SNP-driven cGMP formation, while SNP alone elevated cGMP formation in EC. **$P < 0.001$ versus control ($n = 5$). (C) Immunofluorescence studies on EAhy926 cells showed the binding of antibodies to sGC. No difference in the expression level of sGC was observed between control and thalidomide-treated cells ($n = 5$). (D) Western blots for sGC and β-actin were performed using prepared protein samples for mEC after thalidomide. Immuno-detection of sGC proteins in Western blot revealed that thalidomide had no effect on the expression of sGC in EC ($n = 3$).

The major cavity extends along the length of the catalytic domain. The mouth of the cavity is flanked by two random coils. Our docking studies indicated that thalidomide engages into the deep interior of the mouth touching both the coils and an α-helix. Such binding produces more than 72% block of the available space at this region. We suggest that this docked complex could effectively restrict entry of substrate into the catalytic site of the protein (Figure 8).

Interatomic contact analysis of the sGC model in a complex with thalidomide revealed that, with a distance cut-off less than 1.0 Å, residues Ile 487, Leu 506, Leu 509, Ser 560, Asp 561, Val 563, Met 564, Glu 569, Pro 570, Ile 571, Lys 572 are in contact with thalidomide, whereas with a distance cut-off less than 0.25 Å, all the contacts except Ile 487, Leu 509 and Lys 572 are retained. The details of the interatomic contacts of thalidomide with the carboxy terminus of the modelled sGC are shown in Table 2.

Domain organization

Sequence analysis of the α-subunit of sGC revealed that the residue range 472–659 is mapped by InterPro IPR001054 (adenylate cyclase catalytic domain) and PF00211 (guanylate cyclase domain), and the residue range 481–608 is also mapped by Prosite profile PS50125 (guanylate cyclase domain signature and profile). The NO binding region is spanned by residues 270–471 as indicated by the presence of a haem–NO associated Pfam domain HNOBA PF07701 and InterPro domain IPR011645.

Discussion

Thalidomide, an immuno-modulatory drug, has been shown to inhibit angiogenesis (D'Amato *et al*., 1994). In zebrafish embryos, thalidomide inhibited angiogenesis by depletion of the VEGF receptors, neuropilin-1 and Flk-1 (Yabu *et al*., 2005). Recently, Melchert and List (2007) in their review have discussed the possibility that thalidomide and its analogues exert their effect by suppressing VEGF and bFGF secretion. Evidently, there is more than one way in which thalidomide exerts its effects. Thalidomide has been shown to suppress cellular responses, inhibit various inflammatory cytokines and to alter the bone marrow stromal environment (Melchert

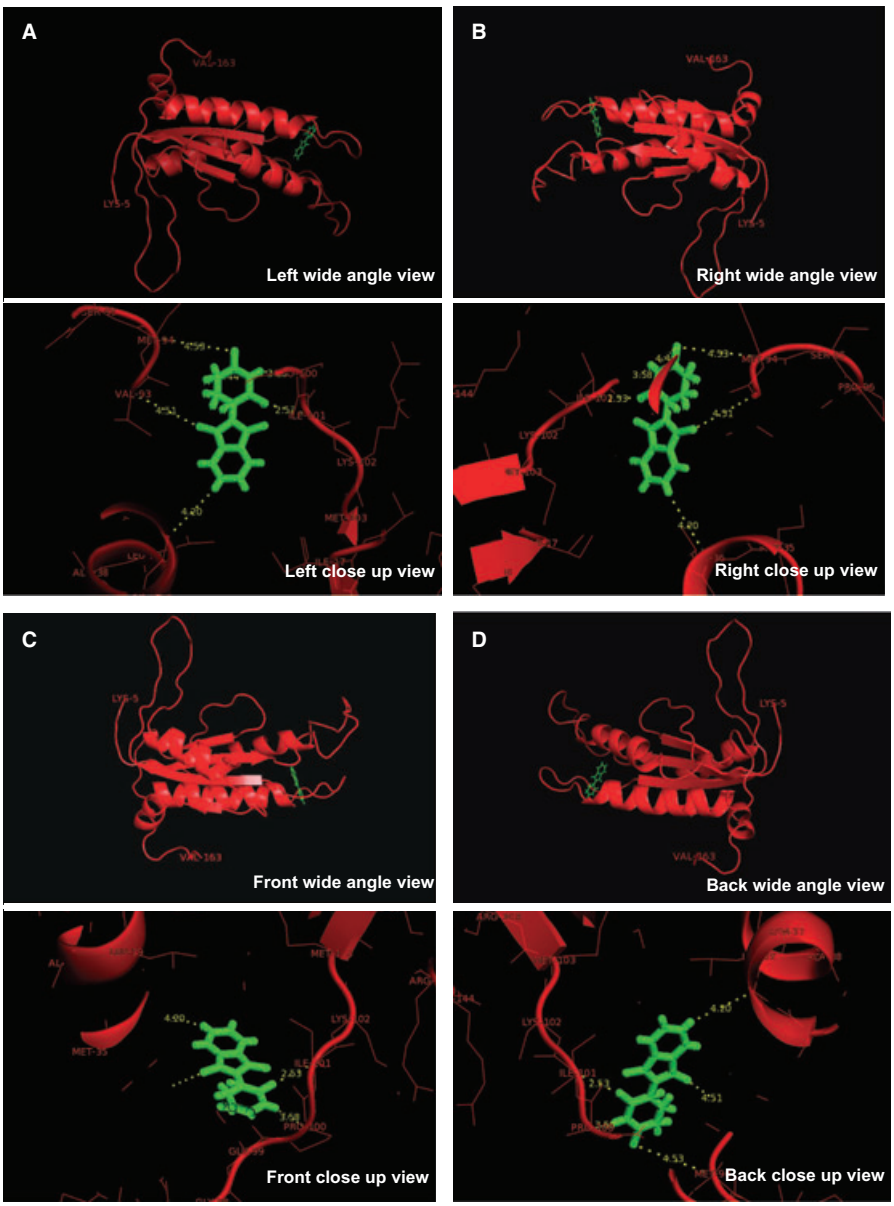

Figure 8 Thalidomide interacts with the catalytic domain of soluble guanylyl cyclase (sGC) to block cGMP formation. The sGC chain of the *in silico* complex was assigned a red colour, while green and yellow have been assigned to thalidomide molecule and molecular bonds between sGC and thalidomide respectively. The residue numbering in this figure corresponds to residue numbering in the partial model of sGC. For example, Pro 100 and Ile 101 in the figure refer to Pro 570 and Ile 571, respectively, in the primary sequence. (A) Left view of the thalidomide and sGC *in silico* complex showing thalidomide interacting with different residues of sGC. Left closed-up view of the complex shows that thalidomide interacts with more than five residues. (B) Right view of the *in silico* complex depicting thalidomide interaction with different residues of sGC. (C) Front view of the *in silico* complex showing interaction of thalidomide with different residues of sGC. (D) Back view of the thalidomide–sGC complex elucidating different point of interaction between thalidomide and sGC.

and List, 2007). However, thalidomide effects are strongly associated with dose and stability of the drug. Thalidomide is poorly soluble in aqueous media in which it degrades, the rate of hydrolysis being dependent on pH and temperature. The work of Chung *et al.* (2004) showed that a plasma sample from multiple myeloma patients over 24 h after their first dose of thalidomide (200 mg) contained 21 $\mu g \cdot mL^{-1}$ (81 μM) of thalidomide. Considering all the stability issues with thalidomide, we aimed to keep the concentration of thalidomide (25–75 $\mu g \cdot mL^{-1}$) for our experiments, close to the therapeutic levels in patients. In a previous report, we have shown that thalidomide blocked NO-mediated angiogenesis by blocking migration of EC (Tamilarasan *et al.*, 2006). In the present work, we expanded our earlier findings and investigated the mechanism of thalidomide action in preventing NO-mediated angiogenic responses. We have previously shown that wound healing in control EC cultures was decreased significantly by thalidomide (Tamilarasan *et al.*, 2006), suggesting that thalidomide worked downstream of NO signalling to inhibit angiogenesis.

The pro-angiogenic effects of NO are widely accepted (Ziche and Morbidelli, 2000), and it exerts its effects by

activation of sGC thereby increasing cGMP production (Ignarro, 1991). The NO/cGMP pathway restored angiogenesis after stroke in rats (Zhang *et al*., 2003). We observed that the levels of cGMP fell after thalidomide treatment, concentration dependently, and that thalidomide also attenuated NO-driven cGMP formation (by SNP) in EC cultures. However, NO delivery, by the NO donor, SNP, failed to restore both endothelial wound healing and ring formation, although thalidomide-induced effects were reversed by 8Br-cGMP, a membrane-permeable analogue of cGMP. These results strongly suggested that the fall in cGMP after thalidomide was the crucial event.

Another way of raising intracellular cGMP levels is to prevent its hydrolysis by PDE-5 (Reffelmann and Kloner, 2003). We used SC to inhibit PDE-5 and found considerable recovery from thalidomide-induced inhibition of EC function (Figures 1A,C and 3A). This PDE inhibitor has been shown to preserve lung angiogenesis and decrease pulmonary vascular resistance (Ladha *et al*., 2005) and, in EC, it stimulated angiogenesis through a protein kinase G/MAPK pathway (Pyriochou *et al*., 2007). All these observations are compatible with the proposal that thalidomide targets the enzymic production of cGMP, that is, targets sGC itself.

The possibility of sGC as the target for thalidomide was further supported by the induction of apoptosis by thalidomide in the EC cultures. Inhibitors of basal sGC are known to promote apoptosis by increasing the caspase activity, release of cytochrome *c* and early events such as reduction of Bcl-2 content and dephosphorylation of Bad at Ser-112 (Flavio *et al*., 2001). Treatment with thalidomide in *ex vivo* and *in vitro* angiogenesis models also provided results compatible with those from the *in vitro* assays. All these results strengthened our suggestion that sGC itself might be the possible target for thalidomide's anti-angiogenic action.

One way of decreasing sGC activity and hence decreasing cGMP levels is by down-regulating the expression of sGC protein, but we found no difference in the level of sGC expression in thalidomide-treated and -untreated EC. The pull-down assays showed clearly that thalidomide did bind to sGC in cells, and our docking studies and further *in silico* analysis have enabled us to suggest a molecular explanation for this binding and the suppression of cGMP production by thalidomide. The homology model that was generated in this study spanned residues 471–633 of the α-subunit of human sGC, a region including the catalytic region of the α-subunit (see Hobbs, 1997; Chang *et al*., 2005). sGC is a heterodimer consisting of two subunits, α and β. Wedel *et al*. (1995) demonstrated that the carboxy termini of both the subunits are involved in dimerization of the enzyme and basal enzymatic activity, and further, the catalytic domain can be functionally expressed separately from the amino terminal regulatory domains. Evidence for the region involved in dimerization of sGC came from studies by Rothkegel *et al* (2007) who tracked mutation-induced alterations of sGC dimerization using a biomolecular fluorescence complementation approach that allowed visualization of sGC heterodimerization in a non-invasive manner in living cells. They suggested that segments spanning the residues 363–372, 403–422 and 440–459 of the α-subunit, and residues 212–222, 304–333 and 381–400 of the β-subunit were involved in the process of heterodimerization and thus expressed in functional sGC. Excluding the region involved in the regulatory activity and dimerization reported in these reports, the catalytic region of the α-subunit of sGC may reside in the residues that have been modelled in this study. Further, sequence analysis also shows that the GC catalytic domain maps to the region that has been modelled. Our docking studies suggested that thalidomide bound to this potential catalytic region.

Further, our experiments with YC-1 (Figure 3C), which is known to bind to an NO-independent, allosteric site, did not show any enhanced activity of sGC during thalidomide treatment. It has been shown that YC-1 is a haem-dependent, but NO-independent, stimulator of sGC (Friebe and Koesling, 1998; Martin *et al*., 2001). In contrast to NO which directly interacts with the haem group of the enzyme, YC-1 does not change the spectral characteristics of the haem moiety of sGC (Friebe and Koesling, 1998; Hoenicka *et al*., 1999). Therefore, NO and YC-1 can both independently, exert their effects through the catalytic domain of sGC, which binds GTP. The inhibitory effects of thalidomide in the presence of YC-1 (Figure 3C) indicated that thalidomide interfered with the catalytic domain and with the NO binding site of sGC.

Although our *in vitro* and *in vivo* results, and the *in silico* analysis all strongly suggest that thalidomide was anti-angiogenic through its depression of cellular cGMP, this may not be the only mechanism operating in our system. For instance, thalidomide may induce apoptosis in EC via other pathways than sGC, as reported elsewhere (Gockel *et al*., 2004). Also, the results of the experiments inhibiting sGC with ODQ and LY83583 along with thalidomide, failed to show complete inhibition of endothelial functions such as endothelial ring formation, which suggested that there may be a cGMP-independent component in the NO-stimulated ring formation in endothelial monolayers. Even though there was a clear reversal after treatment with SC and 8Br-cGMP, we observed a window of inhibition in thalidomide-treated cells, compared to control cells (Figure 1A), clearly suggesting a non-cGMP-related pathway for thalidomide's actions.

In a recent review, Isenberg *et al*. (2009) proposed that inhibitors acting on critical downstream pathways may be more effective than the existing VEGFA–VEGFR2 antagonist for controlling tumour angiogenesis, and therefore sGC would be a key target in anti-angiogenesis therapy. The major observation of the present work is that thalidomide acts downstream of NO by inhibiting sGC action and suppressing cGMP levels to exert its anti-angiogenic function. Therefore, understanding the molecular nature of thalidomide–sGC interaction would facilitate the development of better therapeutic agents for diseases such as cancer, retinopathy and ENL, involving excessive angiogenesis. Based on the knowledge derived from the present work, patients treated with thalidomide should be monitored closely for elevated blood pressure because inhibiting sGC causes hypertension (Fernandes *et al*., 2009). The results of the present study can be used widely for the formulation of combination therapies for the treatment of pathologies involving dysfunctional angiogenesis, by targeting cGMP-mediated pathways

Acknowledgement

This study was financially supported by KB Chandrasekhar Research Foundation.

Conflict of interest

None.

References

Apweiler R, Attwood TK, Bairoch A, Bateman A, Birney E, Biswas M *et al*. (2001). The InterPro database, an integrated documentation resource for protein families, domains and functional sites. *Nucleic Acids Res* **29**: 37–40.

Bairoch A, Apweiler R (2000). The SWISS-PROT protein sequence database and its supplement TrEMBL in 2000. *Nucleic Acids Res* **28**: 45–48.

Berman HM, Westbrook J, Feng Z, Gilliland G, Bhat TN, Weissig H *et al*. (2000). The protein data bank. *Nucleic Acids Res* **28**: 235–242.

Brown J, Reading SJ, Jones S, Fitchett CJ, Howl J, Martin A *et al*. (2000). Critical evaluation of ECV304 as a human endothelial cell model defined by genetic analysis and functional responses: a comparison with the human bladder cancer derived epithelial cell line T24/83. *Lab Invest* **80**: 37–45.

Cardoso CE, Martins ROR, Aucelio RQ (2003). Evaluation of spectrofluorimetric method for the selective determination of thalidomide in pharmaceutical tablets, urine and blood serum. *Microchem J* **77**: 1–7.

Chang FJ, Lemme S, Sun Q, Sunahara RK, Beuve A (2005). Nitric oxide-dependent allosteric inhibitory role of a second nucleotide binding site in soluble guanylyl cyclase. *J Biol Chem* **280**: 11513–11519.

Chung F, Lu J, Palmer BD, Kestell P, Browett P, Baguley BC *et al*. (2004). Thalidomide pharmacokinetics and metabolite formation in mice, rabbits, and multiple myeloma patients. *Clin Cancer Res* **10**: 5949–5956.

Corral LG, Kaplan G (1999). Immunomodulation by thalidomide and thalidomide analogues. *Ann Rheum Dis* **1**: 107–113.

D'Amato RJ, Loughnan MS, Flynn E, Folkman J (1994). Thalidomide is an inhibitor of angiogenesis. *Proc Natl Acad Sci USA* **91**: 4082–4085.

Fernandes D, Sordi R, Pacheco LK, Nardi GM, Heckert BT, Villela CG *et al*. (2009). Late, but not early, inhibition of soluble guanylate cyclase decreases mortality in a rat sepsis model. *J Pharmacol Exp Ther* **328**: 991–999.

Flavio F, Annalisa F, Ivana S, Benedetta T, Francesca B, Claudio S (2001). Control of survival of proliferating L1210 cells by soluble guanylate cyclase and p44/42 mitogen-activated protein kinase modulators. *Biochem Pharmacol* **62**: 319–328.

Finn RD, Tate J, Mistry J, Coggill PC, Sammut SJ, Hotz HR *et al*. (2008). The Pfam protein families database. *Nucleic Acids Res* **36**: 281–288.

Friebe A, Koesling D (1998). Mechanism of YC-1-induced activation of soluble guanylyl cyclase. *Mol Pharmacol* **53**: 123–127.

Gockel HR, Lügering A, Heidemann J, Schmidt M, Domschke W, Kucharzik T *et al*. (2004). Thalidomide induces apoptosis in human monocytes by using a cytochrome *c*-dependent pathway. *J Immunol* **172**: 5103–5109.

Hobbs AJ (1997). Soluble guanylate cyclase: the forgotten sibling. *Trends Pharmacol Sci* **18**: 484–491.

Hoenicka M, Becker EM, Apeler H, Sirichoke T, Schröder H, Gerzer R *et al*. (1999). Purified soluble guanylyl cyclase expressed in a baculovirus/Sf9 system: stimulation by YC-1, nitric oxide, and carbon monoxide. *J Mol Med* **77**: 14–23.

Hulo N, Bairoch A, Bulliard V, Cerutti L, De Castro E, Langendijk-Genevaux PS *et al*. (2006). The PROSITE database. *Nucleic Acids Res* **34**: 227–230.

Ignarro LJ (1991). Heme-dependent activation of guanylate cyclase by nitric oxide: a novel signal transduction mechanism. *Blood Vessels* **28**: 67–73.

Isenberg JS, Martin-Manso G, Maxhimer JB, Roberts DD (2009). Regulation of nitric oxide signalling by thrombospondin 1: implications for anti-angiogenic therapies. *Nat Rev Cancer* **9**: 182–194.

Kolluru GK, Tamilarasan KP, Rajkumar AS, Geetha Priya S, Rajaram M, Saleem NK *et al*. (2008). Nitric oxide/cGMP protects endothelial cells from hypoxia-mediated leakiness. *Eur J Cell Biol* **87**: 147–161.

Ladha F, Bonnet S, Eaton F, Hashimoto K, Korbutt G, Thébaud B (2005). Sildenafil improves alveolar growth and pulmonary hypertension in hyperoxia-induced lung injury. *Am J Respir Crit Care Med* **172**: 750–756.

Laemmli UK (1970). Cleavage of structural proteins during the assembly of the head of bacteriophage T4. *Nature* **15**: 680–685.

Majumder S, Tamilarasan KP, Kolluru GK, Muley A, Nair CM, Omanakuttan A *et al*. (2007). Activated pericyte attenuates endothelial functions: nitric oxide–cGMP rescues activated pericyte-associated endothelial dysfunctions. *Biochem Cell Biol* **85**: 709–720.

Martin E, Lee YC, Murad F (2001). YC-1 activation of human soluble guanylyl cyclase has both heme-dependent and heme-independent components. *Proc Natl Acad Sci USA* **98**: 12938–12942.

Matsuda J, Gotoh M, Gohchi K, Kawasugi K, Tsukamoto M, Saitoh N (1997). Anti-endothelial cell antibodies to the endothelial hybridoma cell line (EAhy926) in systemic lupus erythematosus patients with antiphospholipid antibodies. *Br J Haematol* **97**: 227–232.

Melchert M, List A (2007). The thalidomide saga. *Int J Biochem Cell Biol* **39**: 1489–1499.

Millette E, Lamontagne D (1996). Endothelium-dependent and NO-mediated desensitization to vasopressin in rat aorta. *Br J Pharmacol* **119**: 899–904.

Morris GM, Goodsell DS, Halliday RS, Huey R, Hart WE, Belew RK *et al*. (1998). Automated docking using a lamarckian genetic algorithm and empirical binding free energy function. *J Comput Chem* **19**: 1639–1662.

Mukhopadhyay S, Shah M, Patel K, Sehgal PB (2006). Monocrotaline pyrrole-induced megalocytosis of lung and breast epithelial cells: disruption of plasma membrane and Golgi dynamics and an enhanced unfolded protein response. *Toxicol Appl Pharmacol* **211**: 209–220.

Niemistö A, Dunmire V, Yli-Harja O, Zhang W, Shmulevich I (2005). Robust quantification of *in vitro* angiogenesis through image analysis. *IEEE Trans Med Imaging* **24**: 549–553.

Pearson JM, Vedagiri M (1969). Treatment of moderately severe erythema nodosum leprosum with thalidomide – a double-blind controlled trial. *Lepr Rev* **40**: 111–116.

Peitsch MC (1996). ProMod and Swiss-Model: Internet-based tools for automated comparative protein modelling. *Biochem Soc Trans* **24**: 274–279.

Pyriochou A, Zhou Z, Koika V, Petrou C, Cordopatis P, Sessa WC *et al*. (2007). The phosphodiesterase 5 inhibitor sildenafil stimulates angiogenesis through a protein kinase G/MAPK pathway. *J Cell Physiol* **211**: 197–204.

Randall T (1990). Thalidomide has 37-year history. *JAMA* **263**: 1474.

Reffelmann T, Kloner RA (2003). Therapeutic potential of phosphodiesterase 5 inhibition for cardiovascular disease. *Circulation* **108**: 239–244.

Rothkegel C, Schmidt PM, Atkins DJ, Hoffmann LS, Schmidt HH, Schröder H *et al*. (2007). Dimerization region of soluble guanylate cyclase characterized by bimolecular fluorescence complementation *in vivo*. *Mol Pharmacol* **72**: 1181–1190.

Ryan US (1984). Isolation and culture of pulmonary endothelial cells. *Environ Health Perspect* **56**: 103–114.

Sessa WC (2004). eNOS at a glance. *J Cell Sci* **117**: 2427–2429.

Srinivas G, Anto RJ, Srinivas P, Vidhyalakshmi S, Senan VP, Karunagaran D (2003). Emodin induces apoptosis of human cervical cancer cells through poly(ADP-ribose) polymerase cleavage and activation of caspase-9. *Eur J Pharmacol* **473**: 117–125.

Staton CA, Stribbling SM, Tazzyman S, Hughes R, Brown NJ, Lewis CE (2004). Current methods for assaying angiogenesis *in vitro* and *in vivo*. *Int J Exp Pathol* **85**: 233–248.

Tamilarasan KP, Kolluru GK, Rajaram M, Indhumathy M, Saranya R, Chatterjee S (2006). Thalidomide attenuates nitric oxide mediated angiogenesis by blocking migration of endothelial cells. *BMC Cell Biol* **4**: 7–17.

Tufan AC, Satiroglu-Tufan NL (2005). The chick embryo chorioallantoic membrane as a model system for the study of tumor angiogenesis, invasion and development of anti-angiogenic agents. *Curr Cancer Drug Targets* **5**: 249–266.

Vriend G (1990). WHAT IF: a molecular modeling and drug design program. *J Mol Graphics* **8**: 52–56.

Wedel B, Harteneck C, Foerster J, Friebe A, Schultz G, Koesling D (1995). Functional domains of soluble guanylyl cyclase. *J Biol Chem* **270**: 24871–24875.

Wilhelm SM, Taylor JD, Osiecki LL, Kale-Pradhan PB (2006). Novel therapies for Crohn's disease: focus on immunomodulators and antibiotics. *Ann Pharmacother* **40**: 1804–1813.

Wohlfart P, Malinski T, Ruetten H, Schindler U, Linz W, Schoenafinger K *et al*. (1999). Release of nitric oxide from endothelial cells stimulated by YC-1, an activator of soluble guanylyl cyclase. *Br J Pharmacol* **128**: 1316–1322.

Yabu T, Tomimoto H, Taguchi Y, Yamaoka S, Igarashi Y, Okazaki T (2005). Thalidomide-induced antiangiogenic action is mediated by ceramide through depletion of VEGF receptors, and is antagonized by sphingosine-1-phosphate. *Blood* **106**: 125–134.

Zhang R, Wang L, Zhang L, Chen J, Zhu Z, Zhang Z *et al*. (2003). Nitric oxide enhances angiogenesis via the synthesis of vascular endothelial growth factor and cGMP after stroke in the rat. *Circ Res* **92**: 308–313.

Ziche M, Morbidelli L (2000). Nitric oxide and angiogenesis. *J Neurooncol* **50**: 139–148.